Transient conjugated mixed-convective heat transfer in a vertical annular passage

Y. L. Tsay
Department of Power Mechanical Engineering, National Yuenlin Polytechnic Institute, Huwei, Yuenlin, Taiwan, Republic of China

This study presents a numerical solution of the unsteady conjugated mixed-convective heat transfer in an annular passage resulting from a step change in uniform wall heat flux of the core tube. Results indicate that the dimensionless core tube wall thickness, the wall-to-fluid thermal conductivity ratio, and the wall-to-fluid thermal diffusivity ratio have significant influences on the transient heat transfer characteristics. Effects of the ratio of Grashof number to Reynolds number on the unsteady heat transfer are rather insignificant at the early transient.

Keywords: transient; mixed convection; wall heat capacity; wall conduction

Introduction

Mixed-convection heat transfer in vertical ducts is encountered in many applications, such as in heat exchangers, nuclear reactors, chemical processing equipment, and cooling of modern electronic systems. Recently, the transient characteristics have become more and more important due to the increasing needs of modern technology, especially in relation to the use of automatic control devices for accurate regulation of energy-related systems during power-on and power-off periods, as well as any off-normal surges in a presumed steady, normal operation. Besides, many heat transfer problems involve an interaction between conduction in a solid wall and convection in an adjacent fluid. The thermal conditions along the fluid–wall interface are then not known a priori, but what is known is a thermal boundary condition at the other surface of the solid wall. Thus it is necessary to solve equations for the fluid and the solid wall together. In such situations, the wall conduction and wall heat capacity can have significant effects on the heat transfer characteristics, especially during the transient stage. The main objective of this study is to investigate the effects of wall heat capacity and wall conduction on the transient mixed convection in a vertical annular passage with a sudden change in uniform wall heat flux over the inside surface of the core tube.

Comprehensive reviews of internal-flow mixed convection have been done by Incropera (1986), Aung (1987), and Gebhart et al. (1988). In the following, the literature on mixed convection in vertical ducts is briefly reviewed. Heat transfer in steady laminar mixed convection in a vertical plane channel or tube has been extensively studied in the past. Tao (1960) provided an analytical solution of fully developed mixed convection in a plane channel with heat generation. Quintiere and Mueller (1973) obtained the solution for developing mixed convection between symmetrically heated parallel plates. The predicted Nusselt number was contrasted with the limiting cases of pure free and forced convection. Yao (1983) studied the developing mixed convection in a plane channel with uniform temperature and uniform heat-flux heating. The solutions give the information on various axial length scales to distinguish regions of different convective mechanisms from the developing state to the fully developed state. Steady mixed-convection flow between asymmetrically heated parallel plates was investigated by Aung and Worku (1986a, 1986b, 1987) and Habchi and Acharya (1986). The results show that the asymmetric wall heating can cause a severe distortion in the velocity profile and can exhibit profound influences on the heat transfer process. Heat transfer in steady mixed convection in vertical tubes has been examined numerically and experimentally by numerous researchers. Lawrence and Chato (1966) investigated the effects of heat transfer on the developing velocity and temperature profiles. Marner and McMillan (1970) obtained a numerical solution for fully developed flow in a vertical tube with constant wall temperature. Morton et al. (1989) investigated how recirculation aids and opposes mixed-convection flow. Zeldin and Schmidt (1972) proposed a critical range of Gr/Re of reversal flow for developing or developed flow. Heggs et al. (1990) studied the effects of wall heat conduction on the recirculating mixed convection flow in a vertical tube.

Despite their importance in many practical applications, transient mixed convection flows in vertical channels have received much less attention than the steady flows mentioned above. Shadday (1986) presented a numerical simulation of transient mixed convection flow in vertical tubes. Recently, Lin et al. (1991) studied the unsteady mixed-convection heat transfer in a vertical flat duct by considering the effects of wall heat capacity. Their results show that the wall heat capacity has profound influences on the flow and thermal characteristics. The heat conduction in the wall remains untreated in the analysis, and hence its effect is not known. However, the studies of transient pure natural convection (Joshi 1988) and forced convection (Sucec and Sawant 1984; Sucec 1987; Lin and Kuo 1988) in channels found that both heat conduction in the wall and wall heat capacity play important roles in the transient convective heat transfer.

The lack of information on the transient conjugated mixed-convective heat transfer in channel flow motivates the present work. In this study, a numerical analysis is performed to examine the transient characteristics of mixed convection in a vertical annular passage. Attention is focused on the transient thermal interaction of conduction in the tube wall and the convection in the fluid through the wall–fluid interface.

Address reprint requests to Professor Tsay at the Department of Power Mechanical Engineering, National Yuenlin Polytechnic Institute, Huwei, Yuenlin, Taiwan 63208, Republic of China.

Received 7 September 1993; accepted 4 March 1994

Analysis

The physical model under consideration and the coordinates chosen are depicted in Figure 1. As shown in the figure, two concentric tubes of circular cross section are oriented in the gravitational direction. The outside radius and wall thickness of the core tube are r_i and δ_{wi}, respectively. In addition, the outer tube has inner radius r_o and wall thickness δ_{wo}. Flow entering the annular passage from the upstream region approaches the beginning of the heated section ($x = 0$) with a uniform temperature ($T = T_e$) and corresponding fully developed velocity profile. The whole system is at a uniform temperature T_e. At $t = 0$, a uniform heat flux q_i'' is suddenly subjected to the inner surface of the core tube from $x \geq 0$.

In this study, flow and thermal characteristics in vertical annular passage is considered to be axial symmetric. Besides, only high Peclect number flow is treated here, so the axial conduction in the flow is negligibly small. By introducing the Boussinesq approximation and adopting the boundary-layer approximation, the basic equations in dimensionless form describing the unsteady laminar mixed convection in an annular passage with conduction in the tube walls are as follows:

Continuity equation

$$\frac{\partial(\eta U)}{\partial X} + \frac{\partial(\eta V)}{\partial \eta} = 0 \tag{1}$$

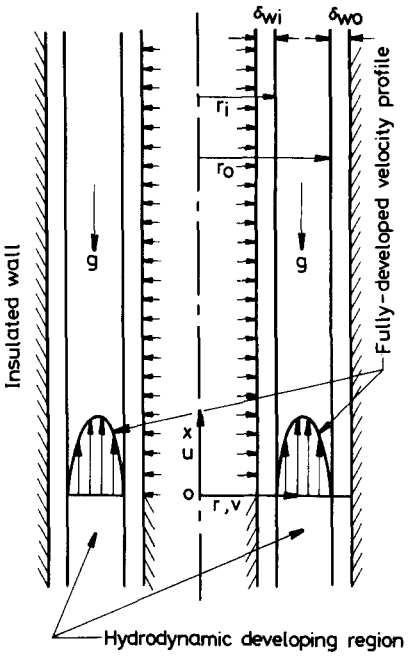

Figure 1 Schematic diagram of the physical system

Notation

a	Coefficient of the finite-difference form of the momentum equation
A_1	Wall-to-fluid heat capacity ratio for plate 1, $\rho_w C_{pw}\delta_1/(\rho_f C_{pf} b)$
A_2	Wall-to-fluid heat capacity ratio for plate 2, $\rho_w C_{pw}\delta_2/(\rho_f C_{pf} b)$
b	Plate spacing
B_i	Dimensionless core tube wall thickness, δ_{wi}/r_o
B_o	Dimensionless outer tube wall thickness, δ_{wo}/r_o
c	Coefficient of the finite-difference form of energy equation
C_p	Specific heat
D_h	Hydraulic diameter, $2(r_o - r_i)$
g	Gravitational acceleration
Gr	Grashof number, $g\beta q_i'' D_h^4/(k_f \nu^2)$
h_i	Local heat transfer coefficient, $q_i''/(T_{wi} - T_e)$
i	Grid position in axial direction
j	Grid position in radial direction
k	Thermal conductivity
K_{wf}	Wall-to-fluid thermal conductivity ratio, k_w/k_f
l	Values for the lth time step
n	Values for the nth iteration
Nu_i	Local Nusselt number, $h_i D_h/k_f$
p_m	Dynamic pressure
P	Dimensionless pressure, $p_m/(\rho \bar{u}_e^2)$
Pr	Prandtl number, ν/α_f
q_i''	Input heat flux to the inside surface of the core tube
q_{ii}''	Heat flux through the core tube wall–fluid interface
Q_{wi}	Dimensionless heat flux through the core tube wall–fluid interface, $r_i q_{ii}''/((r_i - \delta_{wi})q_i'')$
r	Radial coordinate
r_i	Outside radius of the core tube
r_o	Inside radius of the outer tube
r^*	Tube radius ratio, r_i/r_o
Re	Reynolds number, $\bar{u}_e D_h/\nu$
t	Time
T	Temperature
T_e	Inlet or initial temperature
T_{wi}	Core tube wall–fluid interface temperature
u	Axial velocity
$\bar{u}_e$	Mean velocity at entrance
U	Dimensionless axial velocity, $u/\bar{u}_e$
v	Radial velocity
V	Dimensionless radial velocity, $2(1 - r^*)v/(\nu/D_h)$
x	Axial coordinate
X	Dimensionless axial coordinate, $x/(D_h \mathrm{Re})$

Greek symbols

α	Thermal diffusivity
α_{wf}	Wall-to-fluid thermal diffusivity ratio, α_w/α_f
β	Thermal expansion coefficient
γ_H	Heat flux ratio, q_1''/q_2''
δ_{wi}	Core tube wall thickness
δ_{wo}	Outer tube wall thickness
η	Dimensionless radial coordinate, r/r_o
θ	Dimensionless temperature, $(T - T_e)/(q_i'' D_h/k_f)$
ν	Kinematic viscosity
ρ	Density
τ	Dimensionless time, $t/(D_h^2/\nu)$

Subscripts

e	Inlet value
f	Fluid
w	Wall
wi	Core tube wall–fluid interface

Momentum equation

$$\frac{\partial U}{\partial \tau} + U\frac{\partial U}{\partial X} + V\frac{\partial U}{\partial \eta} = -\frac{dP}{dX} + 4(1-r^*)^2\left[\frac{1}{\eta}\frac{\partial}{\partial \eta}\left(\eta\frac{\partial U}{\partial \eta}\right)\right] + \frac{\mathrm{Gr}}{\mathrm{Re}}\theta \tag{2}$$

Energy equation for the fluid

$$\frac{\partial \theta_f}{\partial \tau} + U\frac{\partial \theta_f}{\partial X} + V\frac{\partial \theta_f}{\partial \eta} = \frac{1}{\mathrm{Pr}}4(1-r^*)^2\left[\frac{1}{\eta}\frac{\partial}{\partial \eta}\left(\eta\frac{\partial \theta_f}{\partial \eta}\right)\right] \tag{3}$$

Energy equation for the wall

$$\frac{\partial \theta_w}{\partial \tau} = \frac{\alpha_{wf}}{\mathrm{Pr}}4(1-r^*)^2\left[\frac{1}{\eta}\frac{\partial}{\partial \eta}\left(\eta\frac{\partial \theta_w}{\partial \eta}\right) + \frac{1}{\mathrm{Re}^2}\frac{\partial^2 \theta_w}{\partial X^2}\right] \tag{4}$$

The coefficient of the axial wall conduction term, $1/\mathrm{Re}^2$, is about on the order of 10^{-4} to 10^{-6}. Hence, the wall heat conduction in the axial direction is small relative to that in the radial direction and can be reasonably neglected in the analysis.

The governing equations are subjected to the following initial and boundary conditions:

$$\tau = 0,\ U = \frac{2\left[1-\eta^2-\left(\frac{1-r^{*2}}{\ln r^*}\right)\ln \eta\right]}{(1+r^{*2})+(1-r^{*2})/\ln r^*},\ \theta_f = \theta_w = 0 \tag{5}$$

$$\tau > 0,\ X = 0,\ U = \frac{2\left[1-\eta^2-\left(\frac{1-r^{*2})}{\ln r^*}\right)\ln \eta\right]}{(1+r^{*2})+(1-r^{*2})/\ln r^*},\ \theta_f = \theta_w = 0 \tag{6a}$$

$$\eta = r^* - B_i,\ \frac{\partial \theta_w}{\partial \eta} = -\frac{1}{2K_{wf}(1-r^*)} \tag{6b}$$

$$\eta = r^*,\ U = V = 0,\ \frac{\partial \theta_w}{\partial \eta} = \frac{1}{K_{wf}}\frac{\partial \theta_f}{\partial \eta},\ \theta_w = \theta_f \tag{6c}$$

$$\eta = 1,\ U = V = 0,\ \frac{\partial \theta_w}{\partial \eta} = \frac{1}{K_{wf}}\frac{\partial \theta_f}{\partial \eta},\ \theta_w = \theta_f \tag{6d}$$

$$\eta = 1 + B_o,\ \frac{\partial \theta_w}{\partial \eta} = 0 \tag{6e}$$

In writing the above equations, the following nondimensional variables were used:

$$X = \frac{x}{D_h \mathrm{Re}},\ \eta = \frac{r}{r_o},\ \tau = \frac{t}{D_h^2/\nu},\ U = \frac{u}{\bar{u}_e},$$
$$V = \frac{2(1-r^*)v}{\nu/D_h},\ \theta = \frac{T-T_e}{q_i'' D_h/k_f},\ r^* = \frac{r_i}{r_o},\ P = \frac{P_m}{\rho \bar{u}_e^2},$$
$$\alpha_{wf} = \frac{\alpha_w}{\alpha_f},\ K_{wf} = \frac{k_w}{k_f},\ B_i = \frac{\delta_{wi}}{r_o},\ B_o = \frac{\delta_{wo}}{r_o},$$
$$\mathrm{Re} = \frac{\bar{u}_e D_h}{\nu},\ \mathrm{Gr} = \frac{g\beta q_i'' D_h^4}{k_f \nu^2},\ \mathrm{Pr} = \frac{\nu}{\alpha_f} \tag{7}$$

One constraint to be satisfied in the solution is the overall mass balance at every axial location:

$$\int_{r^*}^{1} (U\eta)\, d\eta = \frac{1-r^{*2}}{2} \tag{8}$$

Equation 8 is used in the solution process to determine the pressure gradient in the flow.

The local Nusselt number is of interest to thermal system design. It is defined as

$$\mathrm{Nu}_i = \frac{h_i D_h}{k_f} = \frac{q_i'' D_h}{(T_{wi}-T_e)k_f} = \frac{1}{\theta_{wi}} \tag{9}$$

Here T_{wi} is the core tube wall–fluid interface temperature.

Another informative parameter for conjugate heat transfer, used to describe the energy transfer into the fluid through the wall–fluid interface, is the dimensionless interfacial heat flux, defined for the core tube wall–fluid interface as

$$Q_{wi} = \frac{r_i q_{ii}''}{(r_i - \delta_{wi})q_i''} = -\frac{r_i k_f (\partial T_f/\partial r)_{r=r_i}}{(r_i-\delta_{wi})q_i''} = -\frac{2(1-r^*)r^*}{r^*-B_i}\left(\frac{\partial \theta_f}{\partial \eta}\right)_{\eta=r^*} \tag{10}$$

where q_{ii}'' is the heat flux through the wall–fluid interface at the core tube wall.

Solution method

In view of the impossibility of obtaining an analytic solution, as indicated in the literature survey, the problem defined by the foregoing equations was solved by finite-difference procedures. The solution is marched in time and in the downstream direction. A fully implicit numerical scheme in which the unsteady energy storage term is approximated by the backward difference, axial convection by upstream difference, and the radial convective and diffusional terms by the central difference is employed to transform the governing equations into finite-difference equations. This system of equations forms a tridiagonal matrix equation that can be solved efficiently by the Thomas algorithm. Note that the matching conditions for the continuities of heat flux imposed at the fluid–wall interfaces were recast in backward difference for $\partial\theta_w/\partial\eta$ and forward difference for $\partial\theta_f/\partial\eta$ at $\eta = r^*$, and backward difference for $\partial\theta_f/\partial\eta$ and forward difference for $\partial\theta_w/\partial\eta$ at $\eta = 1$. Therefore, the solution to the energy equations both in the fluid and pipe walls can be solved simultaneously.

The solution procedures are briefly outlined as follows. For a given time instant and axial location,

(1) Guess $\left(-\frac{dP}{dX}\right)_i^n$.

(2) Solve the finite-difference form of Equation 2 for U.

$$a_{j1}({}^1U^n_{i,j-1}) + a_{j2}({}^1U^n_{i,j}) + a_{j3}({}^1U^n_{i,j+1}) = {}^1\left(-\frac{dP}{dX}\right)_i^n + a_{j4}({}^{1-1}U_{i,j}) + a_{j5}({}^1U^{n-1}_{i,j}\cdot {}^1U_{i-1,j}) + \frac{\mathrm{Gr}}{\mathrm{Re}}({}^1\theta^{n-1}_{i,j}) \tag{11}$$

(3) Numerically integrate the continuity equation for V.

(4) Check if $|\int_{r^*}^{1}(U\eta)d\eta - (1-r^{*2})/2| < 10^{-5}$. If not, repeat procedures (1)–(4).

(5) Solve the finite-difference forms of Equations 3 and 4 for θ_f and θ_w simultaneously:

$$C_{j1}({}^1\theta^n_{i,j-1}) + C_{j2}({}^1\theta^n_{i,j}) + C_{j3}({}^1\theta^n_{i,j+1}) = C_{j4}({}^{1-1}\theta_{i,j}) + C_{j5}({}^1\theta_{i-1,j}) \tag{12}$$

(6) Check if the relative error between two consecutive iterations $n-1$ and n is small enough, i.e., $(|\phi^n - \phi^{n-1}|/\phi^n_{\max}) < 10^{-5}$ for all nodal points where ϕ represents the variables U, θ_f, and θ_w. If not, repeat procedures (1)–(6)

Table 1 Comparison of transient θ_{wi} and Q_{wi} for various grid arrangements for Pr = 5.0, Gr/Re = 500, $K_{wf} = \alpha_{wf} = 50$, $r^* = 0.5$, $B_i = B_o = 0.1$, and $\tau = 0.1217$

	$n_X = 201$	$n_\eta = 121$	$n_X = 151$	$n_\eta = 121$	$n_X = 151$	$n_\eta = 181$
X	θ_{wi}	Q_{wi}	θ_{wi}	Q_{wi}	θ_{wi}	Q_{wi}
0.02	0.0707	0.9217	0.0708	0.9242	0.0705	0.9183
0.06	0.0831	0.8145	0.0834	0.8163	0.0829	0.8109
0.12	0.0857	0.7698	0.0860	0.7701	0.0855	0.7654
0.20	0.0859	0.7627	0.0862	0.7645	0.0856	0.7595

Note: $\Delta\tau_1 = 0.001$ and $\Delta\tau_k = 1.01 \times \Delta\tau_{k-1}$

for the current axial location. If so, repeat procedures (1)–(6) for the next axial location. Apply the above procedures from the entrance to the desired downstream location. Then march the solution from the onset of the transient to the final steady state.

During the program tests, solutions for a typical case with Pr = 5.0, Gr/Re = 500, $K_{wf} = \alpha_{wf} = 50$, $B_i = B_0 = 0.1$, $r^* = 0.5$ were obtained using different space and time intervals to ensure that the solution is grid independent. The results from the computation for various grids are given in Table 1 for a transient state. It is noted that the differences in θ_{wi} and Q_{wi} are always less than 0.7 percent. In the separate computations, a reduction in the first time interval, $\Delta\tau_1$, from 0.001 to 0.0005 results in less than 1 percent difference in Q_{wi}. Accordingly, the 151 × 121 grid with $\Delta\tau_1 = 0.001$ is considered to be suitable for the present study. To further check the adequacy of the numerical scheme employed for the present study, results for the limiting case of forced-convection heat transfer in an annular passage with infinitely thin tube walls were obtained. Excellent agreement was found between the present predictions and those of Heaton et al. (1964). Another limiting case is the transient mixed convection in a vertical flat duct without considering wall conduction. The predicted results agreed well with those of Lin et al. (1991), as shown in Figure 2. This lends support to the employment of the present numerical scheme.

Results and discussion

Inspection of the foregoing analysis reveals that the heat transfer characteristics in the flow depend on seven parameters, namely, the ratio of the Grashof number to Reynolds number Gr/Re, the Prandtl number Pr, the wall-to-fluid thermal conductivity ratio K_{wf}, the wall-to-fluid thermal diffusivity ratio α_{wf}, the core tube-to-outer tube radius ratio r^*, and the dimensionless tube wall thicknesses B_i and B_o. While computations can be performed for any combination of these parameters, the objective here is to investigate the effects of

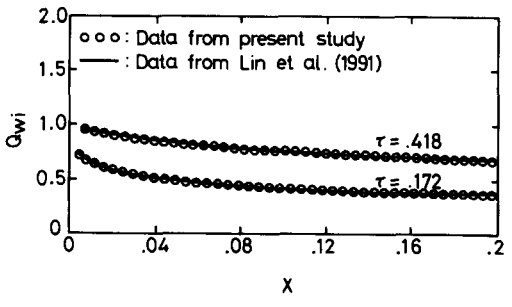

Figure 2 Comparison of the transient distributions of interfacial heat flux with the data from Lin et al. (1991) for Gr/Re = 500, $\gamma_H = 1.0$, and $A_1 = A_2 = 1.0$

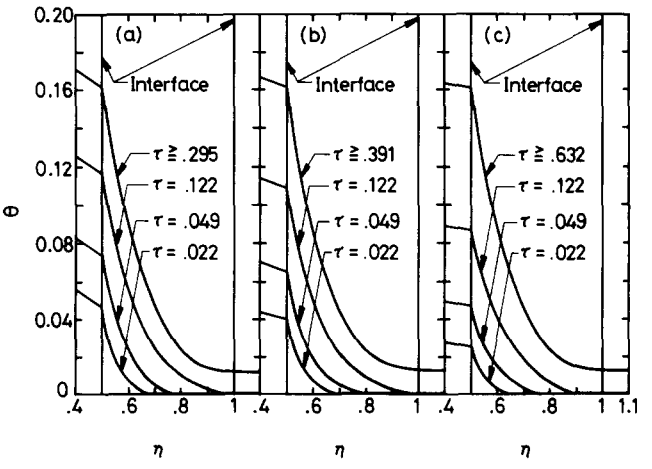

Figure 3 Effects of the wall-to-fluid conductivity ratio on the transient temperature development at $X = 0.2$ for $B_i = 0.1$, $\alpha_{wf} = 50$, Gr/Re = 500, and (a) $K_{wf} = 10$, (b) $K_{wf} = 20$, (c) $K_{wf} = 50$

K_{wf}, α_{wf}, B_i, and Gr/Re on the transient conjugated mixed convection. In particular, a system with water (Pr = 5) flowing through an annular passage with $r^* = 0.5$ and $B_o = 0.1$ is considered. The results are presented for the cases with K_{wf} varying from 10 to 100, α_{wf} from 10 to 200, B_i from 0.05 to 0.2, and Gr/Re from 0 to 5,000.

The temporal development of the temperature profiles for various K_{wf} is illustrated in Figure 3 for a typical case with $B_i = 0.1$, $\alpha_{wf} = 50$, and Gr/Re = 500 at $X = 0.2$. The results indicate that the temperature drop through the core tube wall is significant for $K_{wf} \leq 20$. Accordingly, the wall heat conduction plays a more significant role for a lower K_{wf}. An inspection of the figure reveals that the time period from the start of transient to the steady state is shorter for a system with a smaller K_{wf}. These results can be made plausible by recognizing the fact that a smaller K_{wf} ($= \alpha_{wf}\rho_w C_{pw}/\rho_f C_{pf}$) with α_{wf} fixed means a smaller wall-to-fluid heat capacity ratio ($\rho_w C_{pw}/\rho_f C_{pf}$). Thus, a reduction in K_{wf} results in less energy-storage capacity of the tube wall and, consequently, quickens the evolution of the thermal field. The trend of this outcome agrees with the results of Lin and Kuo (1988) for pure forced-convective heat transfer.

In Figure 4, the unsteady heat-flux distributions along the core tube wall–fluid interface are presented for different values of K_{wf} with $\alpha_{wf} = 50$ and Gr/Re = 500 at various moments in time. At an early transient stage, Q_{wi} is small but rather uniform in the axial direction, except near the beginning of the heated section. Evidently, Q_{wi} is small because the heat input to the system is mostly stored in the core tube wall during this time period, which is known as the thermal lag of the system. The uniformity of Q_{wi} is caused by the dominant radial heat conduction over the axial convection in the flow at small τ. At

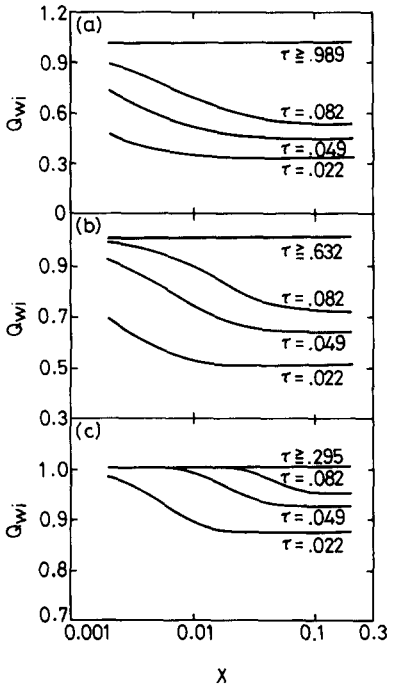

Figure 4 Effects of the wall-to-fluid conductivity ratio on the transient distributions of interfacial heat flux for $B_i = 0.1$, $\alpha_{wf} = 50$, Gr/Re = 500, and (a) $K_{wf} = 100$, (b) $K_{wf} = 50$, (c) $K_{wf} = 10$

any time instant, the axial region where the heat transfer process is significantly influenced by the convection can be approximately estimated as $x/\bar{u}_e \leq t$. And in the dimensionless variable, $x/\bar{u}_e \leq t$ becomes $X \leq \tau$. Hence for $\tau = 0.022$, the Q_{wi} decreases asymptotically with X in the region about $X \leq 0.02$, and beyond that region the Q_{wi} stays rather uniform, as shown in Figure 4. As time goes on, Q_{wi} grows, and the convection-effecting region extends further downstream. Finally, the Q_{wi} gradually rises toward the steady value, $Q_{wi} = 1$.

The transient variations of the local Nusselt number, Nu_i, plotted in Figure 5 are also interested. When K_{wf} is raised from 10 to 100, a substantial change in the transient variation of Nu_i is clearly observed. For $K_{wf} = 100$, the Nusselt number at the initial transient ($\tau = 0.022$) is much higher than that at the steady state. This is because the large K_{wf} makes the interface temperature θ_{wi} still very low at this time instant, according to the definition of the Nusselt number (Equation 9).

Next, the influences of the wall-to-fluid thermal diffusivity ratio ($\alpha_{wf} = \alpha_w/\alpha_f$) on the characteristics of the transient heat transfer are examined. The results shown in Figure 6, indicate that the evolution of the thermal field becomes slower for a system with smaller α_{wf}. This change is due to the fact that for a smaller α_{wf}, heat diffusion in the wall occurs at a slower pace. The variation of α_{wf} results in significant effects on the transient heat transfer characteristics, as shown in Figures 7 and 8.

To investigate the effects of the tube wall thickness on the conjugated heat transfer, the transient distribution of Q_{wi} is displayed in Figure 9 for different values of B_i. As expected, the time required for heat transfer in the system to attain the steady-state condition is shorter for a smaller B_i. This result can be readily understood by recognizing that the thermal resistance and energy-storage capacity of the wall are smaller for a thinner wall, so the heat is easily transported into the fluid. In addition, it is important to note that the thermal lag of the system is still prominent for a system with $B_i = 0.05$ (Figure 9). Consequently, the presence of the tube has a significant influence on the characteristics of unsteady heat transfer, and thus the wall effects cannot be disregarded for transient heat transfer problems.

The last parameter to be discussed is the ratio of the Grashof number to the Reynolds number, Gr/Re. The transient velocity developments for various Gr/Re are presented in Figure 10 for a system with $B_i = 0.1$ and $K_{wf} = \alpha_{wf} = 50$ at $X = 0.2$. For pure forced convection, the velocity remains unchanged with time (Figure 10a). In the presence of the buoyancy force, the flow near the core tube wall is continuously accelerated by the aiding buoyancy force after the initiation of the transient by imposing heat flux to the core tube wall. To maintain the overall mass conservation (Equation 8), flow in the region near the outer tube wall is slowed down. A comparison of Figures 10b and 10c reveals that the distortion of the velocity profiles is more

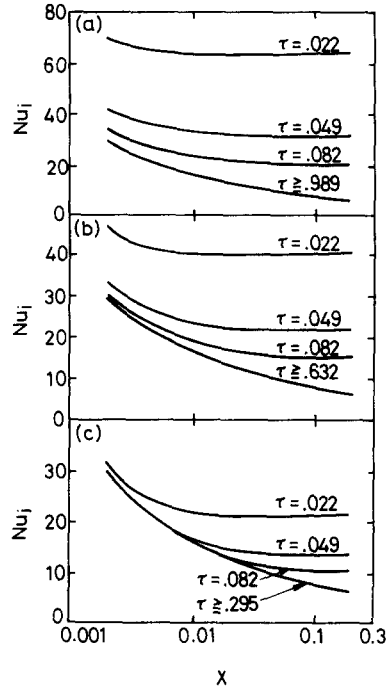

Figure 5 Effects of the wall-to-fluid conductivity ratio on the transient distributions of Nusselt number for $B_i = 0.1$, $\alpha_{wf} = 50$, Gr/Re = 500, and (a) $K_{wf} = 100$, (b) $K_{wf} = 50$, (c) $K_{wf} = 10$

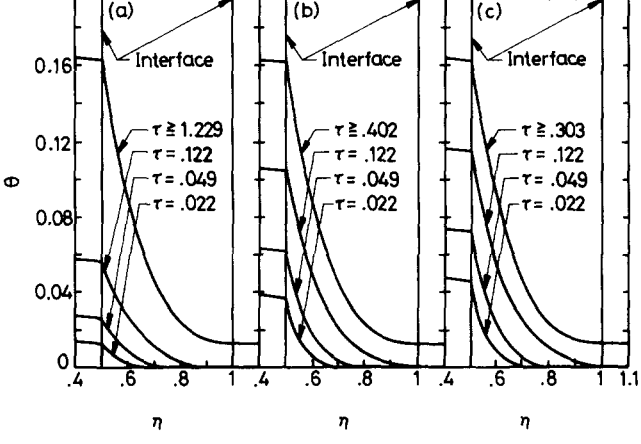

Figure 6 Effects of the wall-to-fluid thermal diffusivity ratio on the transient temperature development at $X = 0.2$ for $B_i = 0.1$, $K_{wf} = 50$, Gr/Re = 500, and (a) $\alpha_{wf} = 20$, (b) $\alpha_{wf} = 100$, (c) $\alpha_{wf} = 200$

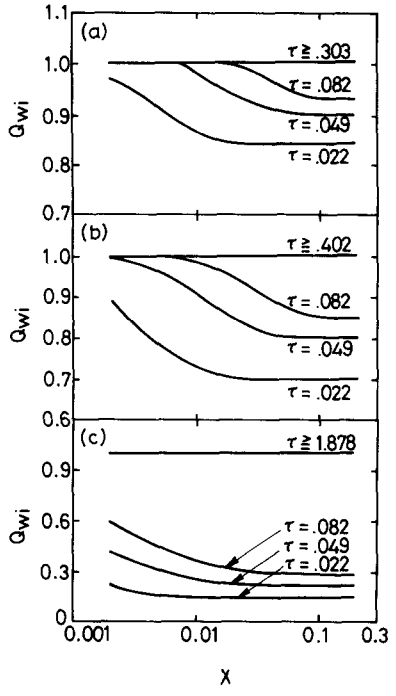

Figure 7 Effects of the wall-to-fluid thermal diffusivity ratio on the transient distributions of interfacial heat flux for $B_i = 0.1$, $K_{wf} = 50$, Gr/Re = 500, and (a) $\alpha_{wf} = 200$, (b) $\alpha_{wf} = 100$, (c) $\alpha_{wf} = 10$

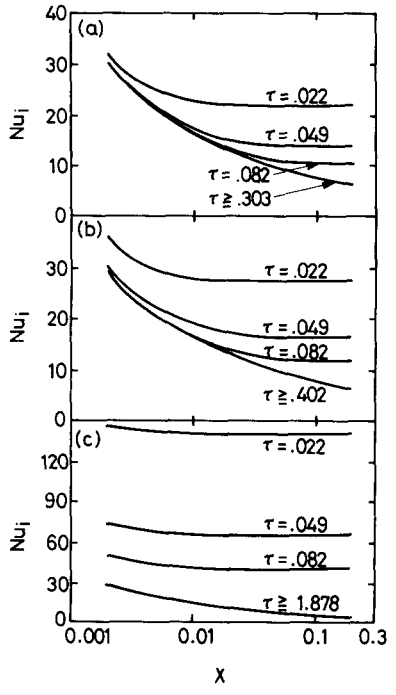

Figure 8 Effects of the wall-to-fluid thermal diffusivity ratio on the transient distributions of Nusselt number for $B_i = 0.1$, $K_{wf} = 50$, Gr/Re = 500, and (a) $\alpha_{wf} = 200$, (b) $\alpha_{wf} = 100$, (c) $\alpha_{wf} = 10$

pronounced, and the steady state occurs earlier for a larger Gr/Re. Also noted is that, near the channel inlet, the distortion in U is small, since the flow is only affected by the buoyancy force over a short distance. In addition, it is interesting to mention that as Gr/Re $\geq$ 8,000, reverse flow occurs in the channel for a typical case with $K_{wf} = \alpha_{wf} = 50$ and $B_i = B_o = 0.1$. Under this situation, a more complicated elliptic flow analysis must be performed.

The effects of Gr/Re on the time variation of temperature profiles are illustrated in Figure 11. As expected, the steady-state temperature is lower for a larger Gr/Re, resulting from the higher velocity in the region near the core tube wall. Also noted in the figure is that the differences in temperature profiles between various Gr/Re are rather insignificant at small τ. This is caused by the dominant radial heat conduction over the axial convection in the flow during the initial transient stage.

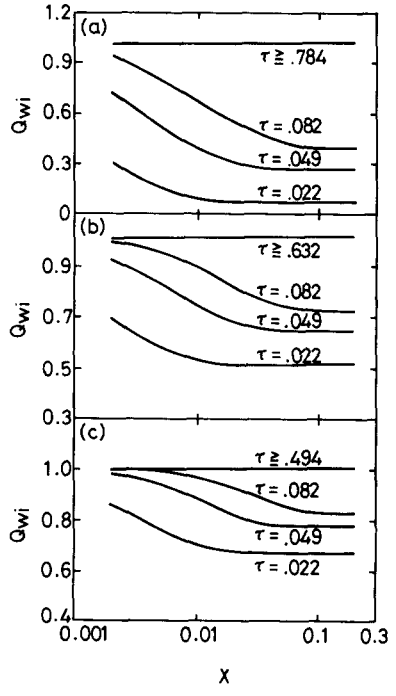

Figure 9 Effects of the dimensionless core tube wall thickness on the transient distributions of interfacial heat flux for $K_{wf} = \alpha_{wf} = 50$, Gr/Re = 500, and (a) $B_i = 0.2$, (b) $B_i = 0.1$, (c) $B_i = 0.05$

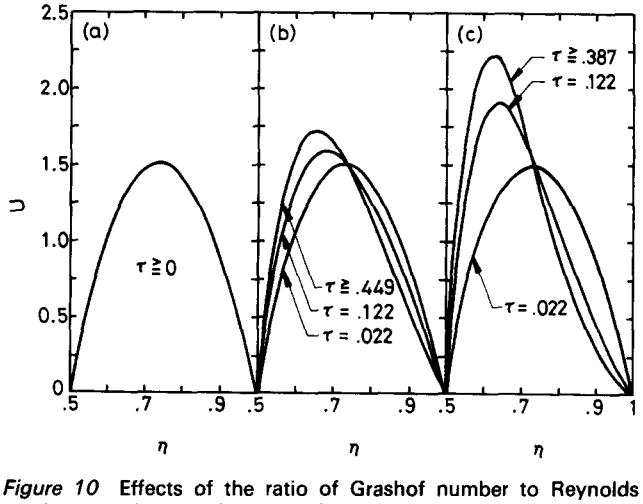

Figure 10 Effects of the ratio of Grashof number to Reynolds number on the transient velocity development at $X = 0.2$ for $B_i = 0.1$, $K_{wf} = \alpha_{wf} = 50$, and (a) Gr/Re = 0, (b) Gr/Re = 2,000, (c) Gr/Re = 5,000

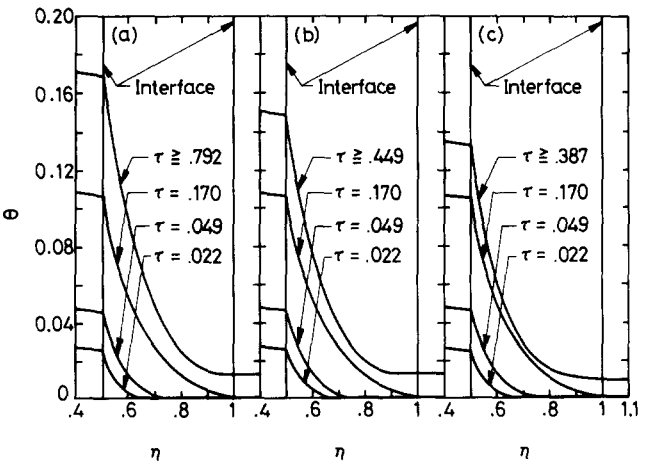

Figure 11 Effects of the ratio of Grashof number to Reynolds number on the transient temperature development at $B_i = 0.1$, $X = 0.2$ for $K_{wf} = \alpha_{wf} = 50$, and (a) Gr/Re = 0, (b) Gr/Re = 2,000, (c) Gr/Re = 5,000

Conclusions

Transient conjugated mixed-convective heat transfer in an annular passage with a uniform heat flux suddenly applied at the inside surface of the core tube wall has been numerically studied. The influences of core tube wall thickness B_i, the wall-to-fluid thermal conductivity ratio K_{wf}, the wall-to-fluid thermal diffusivity ratio α_{wf}, and the ratio of the Grashof number to Reynolds number Gr/Re are examined in great detail. The results obtained in the present study can be briefly summarized as follows.

(1) The wall heat conduction is more significant for a lower K_{wf}.
(2) The variations of K_{wf}, α_{wf}, and B_i result in substantial changes in the transient heat transfer characteristics. The time required for the heat transfer to reach the steady-state condition is longer for the system with larger K_{wf} and B_i or with smaller α_{wf}.
(3) The effects of Gr/Re on the heat transfer characteristics are rather insignificant at the early transient stage.

Acknowledgment

The financial support of this study by the engineering division of the National Science Council, Taiwan, R.O.C., through the contract NSC 81-0401-E-150-505 is greatly appreciated.

References

Aung, W. 1987. Mixed convection in internal flow. In *Handbook of Single-Phase Convective Heat Transfer*, edited by S. Kakac, R. K. Shah, and W. Aung. Wiley, New York, chapter 15

Aung, W. and Worku, G. 1986a. Theory of fully developed combined convection including flow reversal. *ASME J. Heat Transfer*, **108**, 485–488

Aung, W. and Worku, G. 1986b. Developing flow and flow reversal in a vertical channel with asymmetric wall temperature. *ASME J. Heat Transfer*, **108**, 299–304

Aung, W. and Worku, G. 1987. Mixed convection in ducts with asymmetric wall heat fluxes. *ASME J. Heat Transfer*, **109**, 947–951

Gebhart, B., Jaluria, Y., Mahajan, R. L., and Sammakia, B. 1988. *Buoyancy-Induced Flows and Transport*. Hemisphere, Washington, DC

Habchi, S. and Acharya, S. 1986. Laminar mixed convection in a symmetrically or asymmetrically heated vertical channel. *Numer. Heat Transfer*, **9**, 605–618

Heggs, P. J., Ingham, D. B., and Keen, D. J. 1990. The effects of heat conduction in the wall on the development of recirculating combined convection flows in vertical tubes. *Int. J. Heat Mass Transfer*, **33**, 517–528

Incropera, F. P. 1986. Buoyancy effects in double-diffusive and mixed convection flows. In *Proc. 8th Int. Heat Transfer Conf.*, edited by C. L. Tien, V. P. Carey, and J. K. Ferrel, Hemisphere, Washington, DC, Vol. 1, 121–130

Joshi, H. M. 1988. Transient effect in natural convection cooling of vertical parallel channels. *Int. Commun. Heat Mass Transfer*, **15**, 227–238

Lawrence, W. T. and Chato, J. C. 1966. Heat transfer effects on the developing laminar flow inside vertical tube. *ASME J. Heat Transfer*, **88**, 214–222

Lin, T. F. and Kuo, J. C. 1988. Transient conjugated heat transfer in fully developed laminar pipe flows. *Int. J. Heat Mass Transfer*, **31**, 1093–1102

Lin, T. F., Yin, C. P., and Yan, W. M. 1991. Transient laminar mixed convection heat transfer in a vertical flat duct. *ASME J. Heat Transfer*, **113**, 384–390

Marner, W. J. and McMillan, H. K. 1970. Combined free and forced laminar convection in a vertical tube with constant wall temperature. *ASME J. Heat Transfer*, **92**, 559–562

Morton, B. R., Ingham, D. B., Keen, D. J., and Heggs, P. J. 1989. Recirculating combined convection in laminar pipe flows. *ASME J. Heat Transfer*, **111**, 106–113

Quintiere, J. and Mueller, W. K. 1973. An analysis of laminar free and forced convection between finite vertical parallel plates. *ASME J. Heat Transfer*, **95**, 53–59

Shadday, M. A., Jr. 1986. Combined forced/free convection through vertical tubes at high Grashof numbers. *Proc. 8th Int. Heat Transfer Conf.*, edited by C. L. Tien, V. P. Carey, and J. K. Ferrel, Hemisphere, Washington, DC, Vol. 3, 1433–1437

Sucec, J. 1987. Unsteady conjugated forced convection heat transfer in a duct with convection from the ambient. *Int. J. Heat Mass Transfer*, **30**, 1963–1970

Sucec, J. and Sawant, A. 1984. Unsteady, conjugated, forced convection heat transfer in a parallel plate duct. *Int. J. Heat Mass Transfer*, **27**, 95–101

Yao, L. S. 1983. Free and forced convection in the entry region of a heated vertical channel. *Int. J. Heat Mass Transfer*, **26**, 65–72

Zeldin, B. and Schmidt, F. W. 1972. Developing flow with combined forced-free convection in an isothermal vertical tube. *ASME J. Heat Transfer*, **94**, 211–223